Available online at www.sciencedirect.com
SCIENCE DIRECT
Catalysis Today 99 (2005) 291–297
CATALYSIS TODAY
www.elsevier.com/locate/cattod

Electrocatalytic oxidation of methanol: carbon-supported gold–platinum nanoparticle catalysts prepared by two-phase protocol

Jin Luo[a], Mathew M. Maye[a], Nancy N. Kariuki[a], Lingyan Wang[a], Peter Njoki[a], Yan Lin[a], Mark Schadt[a], H. Richard Naslund[b], Chuan-Jian Zhong[a,*]

[a]*Department of Chemistry, State University of New York at Binghamton, Binghamton, NY 13902, USA*
[b]*Department of Geological Sciences, State University of New York at Binghamton, Binghamton, NY 13902, USA*

Available online 15 December 2004

Abstract

This paper describes recent results of an investigation of the electrocatalytic oxidation of methanol at carbon-supported gold and gold–platinum nanoparticle catalysts. The exploration of the bimetallic composition on carbon black support is aimed at modifying the catalytic properties for methanol oxidation reaction (MOR) at the anode in methanol oxidation fuel cells. Gold and gold–platinum nanoparticles of 2–3 nm core sizes with organic monolayer encapsulation were prepared by two-phase protocol. The nanoparticles were assembled on carbon black materials and thermally treated. The electrocatalytic MOR activities were characterized using voltammetric techniques, and were compared with commercial catalysts under several conditions. The results have revealed some initial insights into the catalytic activity of gold–platinum nanoparticle catalysts. Implications of our findings to the design and manipulation of highly-active gold–platinum nanoparticle catalysts for fuel cell applications are also discussed.

Keywords: Electrocatalytic oxidation; Methanol oxidation reaction; Gold–platinum nanoparticle

1. Introduction

Direct methanol fuel cells are increasingly considered as an attractive power source for mobile applications because of the high energy density of methanol, the fuel portability and the easily renewable feature. Currently, however, the energy density (~2000 Wh/kg) and operating cell voltage (0.4 V) for methanol fuel cells are much lower than the theoretical energy density (~6000 Wh/kg) and the thermodynamic potential (~1.2 V) due to poor activity of the anode catalysts and ''methanol cross-over'' to the cathode electrode [1,2], which lead to a loss of about one-third of the available energy at the cathode and another one-third at the anode. Pt-group metals have been extensively studied for both anode and cathode catalysts, but a major problem is the poisoning of Pt by CO-like intermediate species [3–5]. On the cathode, the kinetic limitation of the oxygen reduction is another problem of interest in proton exchange membrane fuel cells operating at low temperature (<100 °C) and in direct methanol fuel cells. The rate of breaking O=O bond to form water strongly depends on the degree of its interaction with the adsorption sites of the catalyst, and competition with other species in the electrolyte (e.g., CH_3OH). For methanol oxidation, the binary PtRu nanoparticle catalyst on carbon support is currently one of the most-studied catalysts [6,7] showing a bifunctional catalytic mechanism, in which Pt provides the main site for the dehydrogenation of methanol and Ru provides the site for hydroxide (OH) and for oxidizing CO-like species to CO_2.

Based on the unique catalytic properties of gold at nanoscale sizes for CO oxidation which have attracted considerable fundamental and practical interests in the last few years [8–16], the electrocatalytic activity of gold nanoparticles for CO and methanol oxidation reactions have recently been explored [17–19]. To further modify the

* Corresponding author. Tel.: +1 607 777 4605.
E-mail address: cjzhong@binghamton.edu (C.J. Zhong).

0920-5861/$ – see front matter © 2004 Elsevier B.V. All rights reserved.
doi:10.1016/j.cattod.2004.10.013

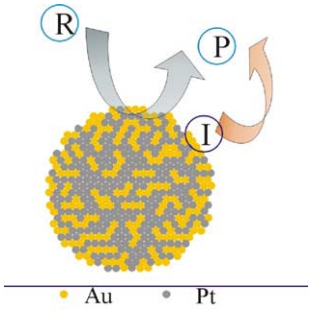

Scheme 1. Schematic illustration of AuPt nanoparticle catalyst and the catalytic reactions on the surface involving adsorption, interfacial reaction, and desorption of reactant (R), intermediate (I) and product (P).

catalytic properties for methanol oxidation reaction (MOR) at the anode in methanol oxidation fuel cells, we envision that the use of bimetallic AuPt composition on carbon black support materials could potentially provide a synergistic catalytic effect and practical utility. The synergistic catalytic effect involves the suppression of adsorbed poisonous species and the change in electronic band structure to modify the strength of the surface adsorption (Scheme 1). While bimetallic AuPt is a known electrocatalyst for oxygen reduction in alkaline fuel cells [14], there have been few reports for the utilization of AuPt nanoparticles with controllable size and composition in fuel cell catalyst applications. Such a study is important mainly because (1) the metal nanoparticles (1–10 nm) undergo a transition from atomic to metallic properties, and (2) the bimetallic composition produces a synergistic effect. With bimetallic Au and Pt systems, Pt functions as main hydrogenation or dehydrogenation sites, and the use of Au together with Pt could speed up the removal of the poisonous species. There are some earlier insights about AuPt bulk alloy catalysts, including the decrease of activation energy for facilitating oxidative desorption and suppressing the adsorption of CO, the sufficiently-high adsorptivity to support catalytic oxidation in alkaline electrolytes, and the important role of OH^{-}_{ads} in alkaline medium and the presence of Au may play a role in reducing the strength of the Pt-OH formation. How these properties operate in the nanoscale is an important area of our study. It has been recently shown [20] that catalysts prepared by impregnation from Pt and Au precursors are similar to those of monometallic Pt catalysts, indicating that the presence of Au did not affect the catalytic performance of Pt in any significant way, because the two metals remain segregated due to their miscibility gap, and only Pt participates in the adsorption of CO and the reactions under consideration. In contrast, catalysts prepared from a PtAu organo-bimetallic cluster precursor exhibited different behavior both in terms of CO adsorption and their catalytic activity, suggesting that Pt and Au remain intimately mixed in the form of bimetallic particles and that the presence of Au modifies the catalytic properties of Pt.

In this paper, we report the results of our preliminary investigation of the electrocatalytic MOR activities of carbon-loaded AuPt nanoparticle catalysts. Unlike some of our earlier electrocatalytic studies in which gold nanoparticles prepared by two-phase protocol [21–24] were assembled on planar glassy carbon electrodes [25–28], the gold and gold–platinum nanoparticles prepared by the same protocol are assembled on carbon black support materials and activated by thermal calcination. We also show the preliminary results of an initial comparison of the electrocatalytic activities of our carbon-supported Au and AuPt nanoparticle catalysts with commercially-available Pt/C and PtRu/C catalysts (E-tek). The electrocatalytic activities were studied in both acidic and alkaline electrolytes. There are three important findings. First, both Au/C and AuPt/C (with a loading of ∼20% metals) exhibited electrocatalytic MOR activities which depend on the electrolyte properties. Second, AuPt nanoparticles with 70–90% Au showed interesting bifunctional electrocatalytic properties in which Pt functions as the main dehydrogenation sites whereas Au speeds up the removal of poisonous CO. And thirdly, some of our AuPt catalysts with ∼80%Au and ∼20% metal loading exhibited at least comparable, and in some cases higher catalytic activities than PtRu catalysts in alkaline electrolytes. The results have provided us with information for assessing the feasibility of the alloy nanoparticle catalysts in fuel cell catalytic applications.

2. Experimental

2.1. Chemicals

Decanethiol (DT, 96%), hydrogen tetrachloroaurate ($HAuCl_4$, 99%), tetraoctylammonium bromide (TOABr, 99%), hydrogen hexachloroplatinate (IV) ($H_2PtCl_6xH_2O$, 99.995%), and NaBH4 were purchased from Aldrich and used as received.

Other chemicals included hexane (99.9%) and toluene (99.8%) from Fisher, and methanol (99.9%) and ethanol (99.9%) from Aldrich. Water was purified with a Millipore Milli-Q water system. Catalysts such as 20% Pt on Vulcan XC-72 (Pt/C) and 20% PtRu on Vulcan XC-72 (PtRu/C) were purchased from E-Tek.

2.2. Catalyst preparation

Gold nanoparticles of 2 nm core size encapsulated with an alkanethiolate monolayer shell (Au) were synthesized by the standard two-phase method [21]. Gold–platinum nanoparticles of 2 nm core size encapsulated with an alkanethiolate monolayer shell (AuPt) were synthesized by a modified two-phase method [24]. Briefly $AuCl_4^{-}$ and $PtCl_6^{2-}$ were first transferred from aqueous solution of $HAuCl_4$ and H_2PtCl_6 into toluene solution using a phase transfer reagent (tetraoctylammonium bromide). Thiols (e.g., decanethiol, DT) was added to the organic solution

at a 4:1 mole ratio (DT/AuPt), and an excess of aqueous $NaBH_4$ was slowly added for the reaction. The produced DT-encapsulated AuPt nanoparticles were subjected to solvent removal, and cleaned using ethanol. The $Au_{81}Pt_{19}$ and $Au_{68}Pt_{32}$ nanoparticles reported in this paper were obtained by controlling the relative feed ratio of $HAuCl_4$ and H_2PtCl_6 in synthesis and the post-synthesis cleaning procedure, details of which will be reported in another paper.

The composition was analyzed using the DCP method, which was performed using an ARL Fisons SS-7 direct current plasma-atomic emission spectrometer (DCP-AES). Measurements were made on emission peaks at 267.59 and 265.95 nm, for Au and Pt, respectively. The nanoparticle samples were dissolved in concentrated aqua regia, and then diluted to concentrations in the range of 1–50 ppm for analysis. Calibration curves were made from dissolved standards with concentrations from 0 to 50 ppm in the same acid matrix as the unknowns. Detection limits, based on three standard deviations of the background intensity, are 0.008 and 0.02 ppm for Au and Pt. Standards and unknowns were analyzed 10 times each for 3 s counts. Instrument reproducibility, for concentrations greater than 100 times the detection limit, results in $<\pm 2\%$ error.

For the assembly of the nanoparticles on carbon support, carbon black XR-72c was first pretreated by suspending in hexane and sonicated for ~6 h at room temperature. A controlled amount of Au or AuPt nanoparticles was added into the suspension. The suspension was sonicated for 30 min, followed by stirring overnight. The product (Au or AuPt supported on carbon) was precipitated out, and was then collected and dried under N_2. The loading of Au or AuPt on carbon support was controlled by the weight ratio of Au or AuPt nanoparticles versus carbon black. The actual loading of metals was determined by TGA and DCP analysis.

2.3. Catalyst treatment

The carbon-loaded nanoparticle catalysts were treated in a tube-furnace under controlled temperatures and atmospheres. A typical protocol included shell removal by heating at 300 °C under 20% O_2/N_2 for 1 h and calcination at 400 °C under 15% H_2/N_2 for 2 h. The carbon-loaded Au or AuPt nanoparticles are denoted as Au/C or AuPt/C.

2.4. Electrode preparation

Glassy carbon (GC) disks (geometric area: 0.07 cm^2) were polished with 0.03 μm Al_2O_3 powders. A typical suspension of the catalysts was prepared by suspending 1 mg catalysts (Au/C, AuPt/C, Pt/C, PtRu/C) in 1 mL 5% Nafion solution, and sonicated for 15 min. The suspension was stable for days. The suspension was then quantitatively transferred to the surface of the polished GC disk. The electrodes were dried overnight at room temperature.

2.5. Measurements

The cyclic voltammetry (CV) measurements were performed at room temperature. All experiments were performed in three-electrode electrochemical cells. All electrolytic solutions were deaerated with high purity argon or nitrogen before the measurement. All potentials are given with respect to the reference electrode of Ag/AgCl saturated KCl. The concentration of methanol was 0.5 M. The cyclic voltammetric measurements were performed by using a microcomputer-controlled potentiostat (Model 273A, PARC).

3. Results and discussion

The discussion of our results is divided into three parts. In the first part, we describe the results obtained for Au/C. This is followed by discussion of the results for AuPt/C. The final part compares the catalytic activities of our catalysts with E-tek's catalysts Pt/C and PtRu/C. Cyclic voltammetric data were used to assess the catalytic activity. Similar data assessment has recently been reported for PtRu/C catalysts [29]. We note that the results reported in the paper are only for limited catalyst systems, and the comparison of the results is thus by no means exhaustive at this stage. We have yet to delineate the optimized alloy composition and calcination condition to control the particle size and surface composition. The particle sizes for the tested catalysts are about 3–5 nm diameters after the thermal treatment of our initial ~2 nm particles. A detailed size and morphological analysis of the catalysts will be reported in another paper.

3.1. Au/C

Fig. 1 shows a typical cyclic voltammetric (CV) curve of Au/C catalysts (17% wt. metals) for methanol oxidation (0.5 M) in alkaline electrolyte (0.5 M KOH).

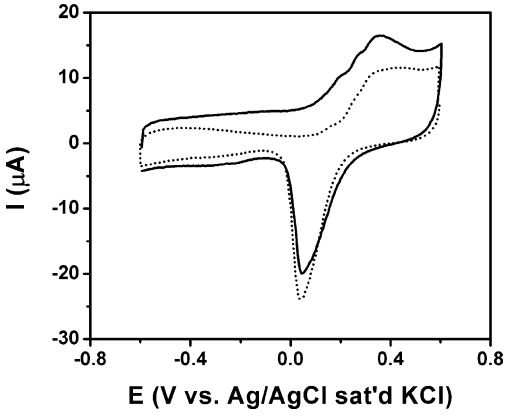

Fig. 1. Cyclic voltammetric curves for a 17% Au/C catalyst (on GC electrode, 0.07 cm^2) in alkaline (0.5 M KOH) electrolytes with (solid curves) and without (dash curves) 0.5 M methanol. Scan rate: 50 mV/s.

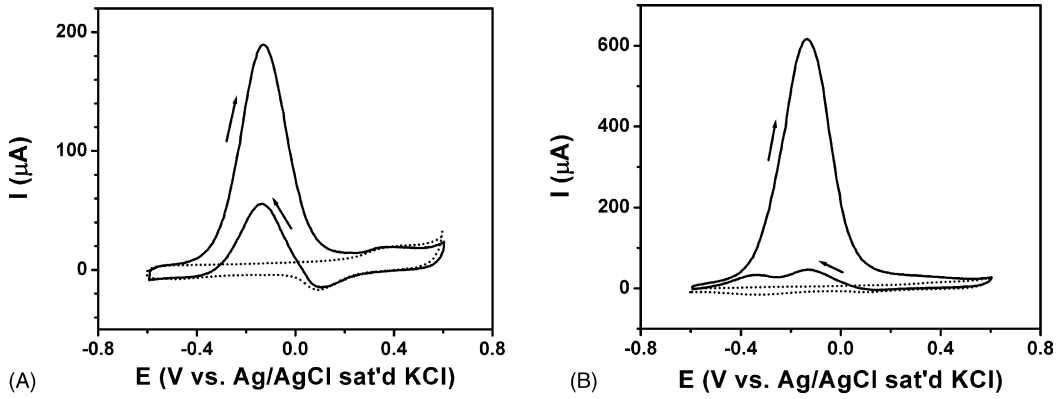

Fig. 2. Cyclic voltammetric curves for a 24% $Au_{81}Pt_{19}$/C catalyst (A) and a 39% $Au_{68}Pt_{32}$/C catalyst (B) (on GC electrode, 0.07 cm^2) in 0.5 M KOH electrolyte with (solid curves) and without (dash curves) 0.5 M methanol. Scan rate: 50 mV/s.

In comparison with the CV curve obtained in the absence of methanol where the gold oxidation–reduction waves are evident (dashed line), the observed increase in the anodic current at ~0.30 V and decrease in cathodic current at 0.05 V are indicative of the oxidation of methanol by the Au catalyst. In terms of peak potentials, the catalytic activity is comparable with those observed for Au nanoparticles directly assembled on GC electrode after electrochemical activation [25–28].

We note however that measurement of the carbon-supported gold nanoparticle catalyst did not reveal any significant electrocatalytic activity for MOR in acidic electrolyte. This observation is consistent with those reported earlier for gold nanoparticles supported on planar electrode surfaces [25]. The results thus indicates that Au nanoparticle catalysts are active only in the presence of hydroxides.

3.2. AuPt/C

Fig. 2 shows a typical set of CV curves obtained for methanol oxidation at AuPt/C catalysts of two different bimetallic compositions in alkaline electrolyte. One composition is $Au_{81}Pt_{19}$/C catalyst with 24% metals loading and the other is $Au_{68}Pt_{32}$/C with 39% metals loading.

In comparison with the data from the control experiment (dashed lines), there is a large anodic wave at −0.13 V, corresponding to the oxidation of methanol. This peak potential is clearly shifted negatively by about 500 mV in comparison with that observed for an Au/C catalyst. The magnitude of the anodic current increases with an increase in the relative Pt composition of the AuPt nanoparticles. Furthermore, a smaller anodic wave is observed at the same potential on the reverse sweep for the $Au_{81}Pt_{19}$/C catalyst, arising from the oxidation of methanol on re-activated catalyst surface [30]. For the $Au_{68}Pt_{32}$/C catalyst, the anodic wave on the reverse sweep is apparently split into two much smaller waves at −0.13 and −0.35 V, respectively. We also note that peak splitting for the anodic wave was observed for AuPt nanoparticles directly assembled on GC electrode surface, which is attributed to the phase segregation of the two metals [31,32]. For example, with 1,9-nonanedithiol(NDT)-linked AuPt nanoparticles assembled on a planar glassy carbon electrode after thermal activation, two anodic waves were observed for methanol oxidation. These two waves, A (0.28 V) and B (−0.08 V), correspond to the reaction sites of Au and Pt, respectively. The current density for wave-B was found to increase with the relative amount of Pt component. In this case, the two metal components in the nanoparticles are likely phase-segregated, which are in contrast to the bimetallic composition for the AuPt nanoparticles supported on carbon black materials. As will be discussed later, the observation of the single anodic wave character in the forward sweep and the differences in the reverse sweep likely reflect a cooperative bimetallic effect of the AuPt nanoparticles on the catalytic reaction.

In acidic electrolyte, the catalytic activity is found to be highly dependent on the alloy composition. For example, while the $Au_{81}Pt_{19}$/C catalyst showed little activity, the $Au_{68}Pt_{32}$/C catalyst showed clear catalytic activity. Fig. 3 shows a typical CV curve obtained for methanol oxidation at the $Au_{68}Pt_{32}$/C (39% metals) catalyst in an acidic electrolyte. In comparison with data from the control

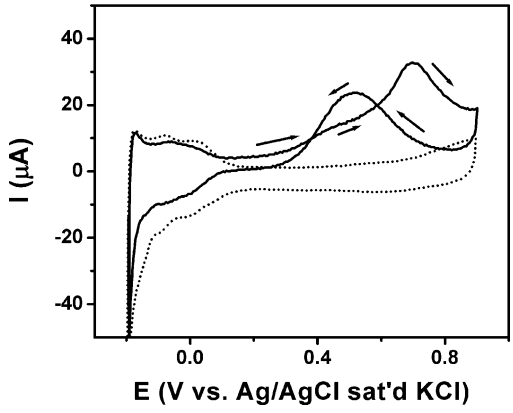

Fig. 3. Cyclic voltammetric curves for a 39% $Au_{68}Pt_{32}$/C catalyst (on GC electrode, 0.07 cm^2) in 0.5 M H_2SO_4 with (solid curve) and without (dash curve) 0.5 M methanol. Scan rate: 50 mV/s.

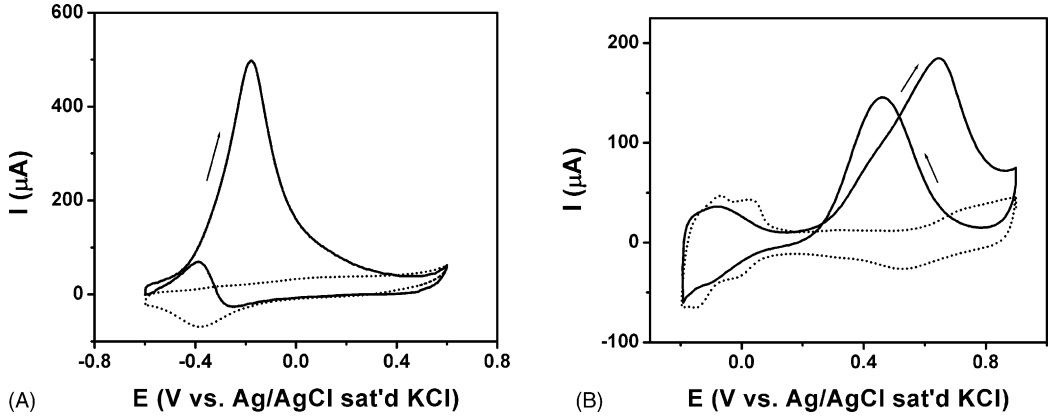

Fig. 4. Cyclic voltammetric curves for methanol oxidation at E-tek's 20% Pt/C catalysts (on GC electrode, 0.07 cm^2) in 0.5 M KOH (A) and 0.5 M H_2SO_4 (B) with (solid curves) and without (dash curves) 0.5 M methanol. Scan rate: 50 mV/s.

experiment (dashed line), there are two important findings. First, in the 0.2–0.8 V potential range, an anodic wave at 0.7 V is evident, which corresponds to the oxidation of methanol. In the reverse sweep, the anodic wave is observed at a less positive potential (+0.5 V), arising from the oxidation of methanol on re-activated catalyst surface [30]. Secondly, in the −0.2 to 0.1 V potential range, the features characteristic of hydrogen adsorption waves and hydrogen evolution current characteristic of Pt component is clearly modified by the presence of Au component. As it will be discussed later, these two findings indicate that the operation of the bimetallic composition of the AuPt nanoparticles in the electrocatalytic reaction.

3.3. Comparisons of electrocatalytic activities

The above electrochemical data are compared with those from commercially-available catalysts, namely E-tek's Pt and PtRu catalysts. For the comparison with our Au/C and AuPt/C catalysts, as reported in this paper, we have examined E-tek's 20%Pt/C and 20% PtRu/C catalysts under the same condition.

Fig. 4 shows a typical set of CV curves for methanol oxidation at E-tek's 20%Pt/C catalysts in both alkaline and acidic electrolytes. As indicated by the anodic waves, the electrocatalytic activity is evident in both electrolytes.

Fig. 5 shows another set of CV curves for methanol oxidation at E-tek's 20%PtRu/C catalysts in both alkaline and acidic electrolytes. As indicated by the anodic waves, the basic electrocatalytic characteristic is largely similar to that for the 20%Pt/C catalyst, except for subtle differences in magnitude of the peak current.

In the above two sets of data for the E-tek's catalysts, we have observed characteristics qualitatively similar to those observed for the AuPt/C catalysts. There are however important differences upon a close examination. For the anodic waves of MOR, we observe differences on the reverse sweeps in terms of the relative peak potential and current. The re-activation of the surface catalytic sites after the anodic sweep is likely modified by the presence of Au in the catalyst, which leads to the shift of the peak potential to a more positive potential. For the hydrogen adsorption/ reduction voltammetric characteristics, we observe changes in peak shapes and relative currents of the adsorption/

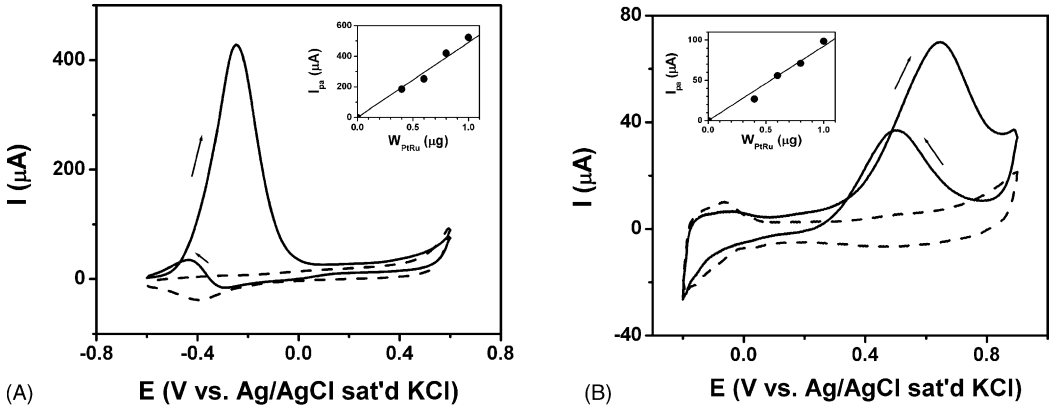

Fig. 5. Cyclic voltammetric curves for methanol oxidation at E-tek's 20% PtRu/C catalysts (on GC electrode, 0.07 cm^2) in 0.5 M KOH (A) and 0.5 M H_2SO_4 (B) with (solid curves) and without (dash curves) 0.5 M methanol. Scan rate: 50 mV/s. The plots of peak current versus the amount of catalysts loaded on the GC electrode surface are included as insets.

Table 1
Comparison of MeOH (0.5 M) oxidation peak potential (E_{pa}) and peak current (i_{pa})

Catalyst	wt.% Mt	M_1:M_2	0.5 M KOH		0.5 M H_2SO_4	
			E_{pa} (mV)	i_{pa} (mA/cm^2/mg Mt)	E_{pa} (mv)	i_{pa} (mA/cm^2/mg Mt)
Pt/C (E)	20% Pt		−179 (Rev.−390)	8875	+645 (Rev. 458)	3304
PtRu/C (E)	20% PtRu	1:1	−248 (Rev.−438)	7643 (Rev. 652)	+644 (Rev. 502)	1250 (Rev.659)
Au/C	17% Au		+357	349	–	–
AuPt/C	24% AuPt	81:19	−131 (Rev.-137)	2820	∼+609	∼113
AuPt/C	39% AuPt[a]	68:32	−136 (Rev.-127)	5643	+693(Rev.521)	304

Electrode coverage: 57 μg catalyst/cm^2; Rev.: reversed scan; electrode area: 0.07 cm^2; scan rate: 50 mV/s; ref. electrode: Ag/AgCl, saturated KCl.
[a] In the catalysts, there could be a small fraction of salt residuals left from the synthesis. M_1:M_2 is the atomic ratio of Au vs. Pt for AuPt and Pt vs. Ru for PtRu; Mt: total metals; E: E-tek product.

desorption and the bulk reduction waves. This observation again reflects the surface modification of the catalysts by the presence of Au. For a quantitative comparison of the data, we have also measured the peak current versus the amount of catalysts loaded onto the electrode surface. The result displays basically a linear relationship (see inserts in Fig. 5). This indicates comparability of data because the catalysts loading of Au/C and AuPt/C on the electrode surface fall in the linear range. Table 1 summarizes the above data for the different catalysts.

While the comparison is preliminary at this stage because we have only limited sets of bimetallic compositions and metal loading for the Pt/C, PtRu/C, Au/C and AuPt/C catalysts, it nevertheless provides us valuable information for an initial assessment of the alloy catalysts. By comparing peak potentials and peak currents, we can reach two important preliminary conclusions. First, both peak potential and current for the electrocatalytic oxidation of methanol are significantly affected by the alloy composition in the alkaline electrolyte. The peak potentials for the AuPt nanoparticles are slightly more positive than that for the Pt/C (by ∼+40 mV) and that for the PtRu/C (by ∼+100 mV). The peak current density of the AuPt, after being normalized to the total metal loading, is smaller than both of the E-tek's catalysts by a factor of 2–3. This observation indicates that there is a major enhancement in comparison with that of Au/C catalysts in terms of the peak potential (by ∼−500 mV) and the peak current (by ∼20×). The presence of a small fraction of Pt in the Au-based bimetallic nanoparticles significantly modified the catalytic properties.

Second, we have observed the display of a significant electrocatalytic activity for MOR at the AuPt/C catalysts in the acidic electrolyte. This observation is in sharp contrast to the little activity observed for Au/C. Depending on the relative composition of Pt component in the bimetallic nanoparticles, the peak potential is only slightly lower or higher than the Pt/C or PtRu/C catalysts (by −30 ∼ + 50 mV). We note however that the peak current is less by a factor of 10–20 (depending on the Pt composition) than the Pt/C or PtRu/C catalysts. While a detailed characterization is needed, it is clear that the bimetallic AuPt composition played a significant role in the observed modification of the catalytic properties.

As stated earlier, the catalytic modification of the bimetallic composition is in fact further reflected by the remarkable difference of the voltammetric characteristic observed in the reverse scan, especially in the alkaline electrolyte. For Pt/C and Pt/Ru/C, the reverse wave for alkaline electrolyte occurs at a potential less positive than the forward wave by ∼200 mV. In contrast, the reverse wave for the AuPt/C occurs at essentially the same potential as for the wave in the forward sweep. The relative peak current of the reverse/forward wave is also found to be dependent on Au% in the bimetallic nanoparticle. The oxides formed on the catalyst surface at the potential beyond the anodic peak potential in the positive sweep are reduced in the reverse sweep [30]. Poisonous CO species formed on Pt surface can also be removed in the reversed sweep. As such, the observation of the more positive potential for the reverse wave likely reflects the bimetallic effect on the re-activation of the catalyst surface after the anodic sweep, a scenario that is under further investigation using spectroscopic techniques.

4. Conclusions

The initial results have indicated that the bimetallic AuPt composition can significantly modify the electrocatalytic properties for the MOR reaction. It is important to note that the AuPt catalyst composition and its calcination treatment are by no means optimised at this stage. Our on-going work aimed at a detailed delineation of the activity correlation with composition, size, and calcination conditions via spectroscopic and microscopic characterizations. With such a further systematic study, we believe that AuPt nanoparticle catalysts are potentially viable candidates for use as fuel cell catalysts under a number of conditions. One of the important properties under investigation is the miscibility gap of Au and Pt known for bulk bimetallic AuPt metals [33]. It is known that bulk AuPt metals with a composition below ∼80%Au could lead to phase segregation. The understanding of how this well-known phenomenon for the bulk AuPt metals is operative at the nanoscale under different temperatures and the development of the ability to control it are some of the key areas of our research towards

manipulating the catalytic activities. These aspects are important particularly in view of the unique phenomenon of melting point decrease of particles at nanoscale, which could lead to very different alloy and phase properties.

Acknowledgements

This work was supported in part by the National Science Foundation (CHE 0316322), the Petroleum Research Fund administered by the American Chemical Society, and the GROW of World Gold Council. M.M. Maye thanks the Department of Defense for the National Defense Science & Engineering Graduate Fellowship support sponsored by ARO.

References

[1] X.M. Ren, P. Zelenay, S. Thomas, J. Davey, S. Gottesfeld, J. Power Sources 86 (2000) 111.
[2] D. Chu, R. Jiang, Solid State Ionics 148 (2002) 591.
[3] U.A. Paulus, U. Endruschat, G.J. Feldmeyer, T.J. Schmidt, H. Bonnemann, R.J. Behm, J. Catal. 195 (2000) 383.
[4] E. Antolini, Mater. Chem. Phys. 78 (2003) 563.
[5] G.Q. Lu, A. Wieckowski, Curr. Opin. Coll. Interf. Sci. 5 (2000) 95.
[6] E. Reddington, A. Sapienza, B. Gurau, R. Viswanathan, S. Sarangapani, E.S. Smotkin, T.E. Mallouk, Science 280 (1998) 1735.
[7] R.X. Liu, E.S. Smotkin, J. Electroanal. Chem. 535 (2002) 49.
[8] M. Haruta, Catal. Today 36 (1997) 153.
[9] M. Haruta, M. Date, Appl. Catal. A 222 (2001) 427.
[10] G.C. Bond, D.T. Thompson, Gold Bull. 33 (2000) 41.
[11] C.W. Corti, R.J. Holliday, D.T. Thompson, Gold Bull. 35 (2002) 111.
[12] Gold 2003—New Industrial Applications for Gold, Proceeding Volume, World Gold Council, 2003.
[13] M. Valden, X. Lai, D.W. Goodman, Science 281 (1998) 1647.
[14] D. Cameron, R. Holliday, D. Thompson, J. Power Sources 118 (2003) 298.
[15] D.R. Rolison, Science 299 (2003) 1698.
[16] T.F. Jaramillo, S.H. Baeck, B.R. Cuenya, E.W. McFarland, J. Am. Chem. Soc. 125 (2003) 7148.
[17] C.J. Zhong, M.M. Maye, J. Luo, L. Han, N.N. Kariuki, in: V.M. Rotello (Ed.), Nanoparticles: Building Blocks for Nanotechnology, Kluwer Academic Publishers, 2004, pp. 113–144, Chapter 5.
[18] C.J. Zhong, J. Luo, M.M. Maye, L. Han, N.N. Kariuki, in: B. Zhou, S. Hermans, G.A. Somorjai (Eds.), Nanotechnology in Catalysis, vol. 1, Kluwer Academic/Plenum Publishers, 2004, pp. 222–248 Chapter 11.
[19] C.J. Zhong, M.M. Maye, Adv. Mater. 13 (2001) 1507.
[20] C. Mihut, C. Descorme, D. Duprez, M.D. Amiridis, J. Catal. 212 (2002) 125.
[21] M. Brust, M. Walker, D. Bethell, D.J. Schiffrin, R. Whyman, J. Chem. Soc. Chem. Commun. (1994) 801.
[22] M.M. Maye, W.X. Zheng, F.L. Leibowitz, N.K. Ly, C.J. Zhong, Langmuir 16 (2000) 490.
[23] M.M. Maye, C.J. Zhong, J. Mater. Chem. 10 (2000) 1895.
[24] M.J. Hostetler, C.J. Zhong, B.K.H. Yen, J. Anderegg, S.M. Gross, N.D. Evans, M.D. Porter, R.W. Murray, J. Am. Chem. Soc. 120 (1998) 9396.
[25] Y. Lou, M.M. Maye, L. Han, J. Luo, C.J. Zhong, Chem. Commun. (2001) 473.
[26] J. Luo, M.M. Maye, Y. Lou, L. Han, M. Hepel, C.J. Zhong, Catal. Today 77 (2002) 127.
[27] J. Luo, Y.B. Lou, M.M. Maye, C.J. Zhong, M. Hepel, Electrochem. Comm. 3 (2001) 172.
[28] M.M. Maye, J. Luo, Y. Lin, M.H. Engelhard, M. Hepel, C.J. Zhong, Langmuir 19 (2003) 125.
[29] E.R. Fachini, R. Diaz-Ayala, E. Casado-Rivera, S. File, C.R. Cabrera, Langmuir 19 (2003) 8986.
[30] T. Page, R. Johnson, J. Hormes, S. Noding, B. Rambabu, J. Electroanal. Chem. 485 (2000) 34.
[31] M.M. Maye, J. Luo, W.-B. Chan, L. Han, N. Kariuki, H.R. Naslund, M.H. Engelhard, Y. Lin, R. Sze, C.J. Zhong, in: P. Knauth, J.-M. Tarascon, E. Traversa, H.L. Tuller (Eds.), Solid-State Ionics-2002 (MRS Symposium Proceedings Volume 756), Materials Research Society, 2003. FF6.2.
[32] M.M. Maye, J. Luo, L. Han, N. Kariuki, C.J. Zhong, Gold Bull. 36 (2003) 75.
[33] V. Ponec V, G.C. Bond (Eds.), Catalysis by Metals and Alloys, Elsevier, 1995.